

## Disorder, defects, and optical absorption in *a*-Si and *a*-Si:H

Simone Knief and Wolfgang von Niessen

*Institut für Physikalische und Theoretische Chemie, Technische Universität Braunschweig, Hans-Sommer-Straße 10,  
D-38106 Braunschweig, Germany*

(Received 23 December 1998)

In this paper we present the optical properties of various structural models for *a*-Si and *a*-Si:H. We discuss how topological disorder, hydrogen content, and different types of defects (dangling bonds and floating bonds) influence the shape of the optical-absorption spectrum and the position of the Urbach edge. The absorption behavior is characterized by the joint density of states. The band gaps are obtained via the Tauc plot. The principal structure of the optical absorption spectrum is determined mainly by the degree of topological disorder and the amount of hydrogen. The presence of defects gives rise to tail absorption. Dangling bonds affect the optical properties more than floating bonds do. [S0163-1829(99)08319-8]

### I. INTRODUCTION

During the last 20 years the physics and technology of amorphous silicon (*a*-Si) and its hydrogenated form (*a*-Si:H) have reached a degree of maturity which has made possible the use of these materials in an increasing number of applications. To produce materials of high device quality, a detailed analysis of the relation between the electronic properties and the network structure is necessary. The knowledge of the optical properties also provides useful insight into how topological disorder and defects influence the properties of amorphous semiconductors. In a previous paper we studied the electronic density of states (DOS) and the localization behavior of the states for different structural models for *a*-Si and *a*-Si:H.<sup>1</sup> In this paper we focus our attention on the optical properties of these structural models.

Whereas the optical spectrum of *c*-Si consists of two peaks and terminates abruptly at the band edges, the spectrum of the amorphous form has a rather diffuse structure. The imaginary part of the dielectric constant contains only a single broad asymmetric peak which extends into the gap region. The width of this tail depends on the degree of disorder and the bonding character of the atoms.

The absorption spectra of *a*-Si and *a*-Si:H generally consist of three ranges characterized by their photon energy dependence.<sup>2</sup> They are called high-energy absorption, Urbach region, and tail absorption. The high-energy region is characterized by optical-absorption coefficients larger than  $10^4 \text{ cm}^{-1}$ . The structure of the optical spectrum in this energy range is caused by transitions between extended electronic states, just as those which occur in the corresponding crystalline structures. It is generally believed that the absorption coefficient in the high-energy region shows a parabolic dependence on the energy. An exponential dependence on the energy is observed for absorption coefficients  $\alpha \leq 10^3 \text{ cm}^{-1}$ . This part of the optical spectrum is called the Urbach region, and extends over several orders of magnitude in the absorption coefficient  $\alpha$ .<sup>3</sup> This energy region is characterized by transitions between localized electronic states in one band tail and extended states in the other band.<sup>4</sup> On account of the broader tail of the valence band (VB), the number of transitions from localized states in the VB to ex-

tended states in the conduction band (CB) exceeds the number of transitions between extended states in the VB and localized states in the tail of the CB. The third part of the optical spectrum is located below the Urbach region, and is called tail or defect absorption. This energy range belongs to transitions involving defect states which are localized in the vicinity of the Fermi level.

For amorphous semiconductors it is generally assumed that the exponential absorption tail is directly related to a similar exponential tail of the DOS of either one of the two energy bands.<sup>2</sup> The absorption coefficient  $\alpha$  can be written in the form

$$\alpha(\hbar\omega) = M^2(\hbar\omega) \int D_V(E) D_C(E + \hbar\omega) dE. \quad (1)$$

The integral is the joint density of states (JDOS) which integrates over all pairs of states in the valence band and the conduction band separated by a constant energy  $\hbar\omega$ . Jackson and co-workers<sup>5,6</sup> used experimentally obtained DOS distributions of the VB and CB to determine the JDOS and to study the energy dependence of the dipole matrix element  $M(E)$  for interband absorption in *c*-Si and *a*-Si:H. Their results indicate that the value of the matrix element is nearly independent of the photon energy in the range from 1.5 to 3.4 eV, and decreases rapidly at higher energies. For photon energies below 1.5 eV the value of  $M(E)$  is slightly higher than in the range 1.5–3.4 eV. Due to this relative energy independence of the matrix element, the main contribution to the absorption coefficient of amorphous semiconductors is given by the convolution of the VB and CB. For amorphous silicon it is generally assumed that the VB tail, with a width of 40–60 meV, is broader than the tail of the CB (10–30 meV), and therefore dominates the absorption edge in the optical spectrum.<sup>7</sup>

The slope of the Urbach tail  $E_0$  defined as  $E_0 = \partial\hbar\omega / \partial \ln \alpha$  can also be used to characterize the degree of disorder in amorphous systems.<sup>8,2</sup> For unhydrogenated amorphous silicon the value of the Urbach slope varies between 60 and 160 meV depending on the preparation conditions. The experiment demonstrates that in *a*-Si the slope of the Urbach tail increases with the defect concentration. The in-

roduction of hydrogen has the opposite effect, i.e., the value of the Urbach slope decreases with an increasing amount of hydrogen.<sup>7</sup>

There is no pronounced feature in the optical absorption spectrum of an amorphous semiconductor which can be directly related to an optical gap  $E_g$ . Therefore,  $E_g$  can only be defined in terms of an extrapolation of the energy bands. Several methods are currently in use to define an optical gap in amorphous semiconductors, and have been discussed controversially. The simplest one is to consider  $E_g$  as the energy corresponding to an absorption coefficient  $\alpha$  of  $10^4 \text{ cm}^{-1}$ . The band gap obtained via this procedure is called the iso-absorption gap  $E_{04}$ .<sup>9,10</sup> Another useful definition of the optical gap is the Tauc plot.<sup>11</sup> In almost all investigated amorphous semiconductors, the optical-absorption spectrum above  $\alpha=10^4 \text{ cm}^{-1}$  follows the empirical law

$$[\hbar\omega\alpha(\hbar\omega)]^{1/2}=B^{1/2}(\hbar\omega-E_{Tauc}) \quad (2)$$

under the assumption that both the VB and CB have parabolic band edges.  $B^{1/2}$  includes information on the convolution of the two energy bands and the matrix element of optical transitions. The value of the optical gap ( $E_{Tauc}$ ) can be obtained from this relation by extrapolating the absorption coefficient to zero absorption. Jackson *et al.*<sup>5</sup> compared the optical gaps for *a*-Si:H obtained with different criteria, and found that the Tauc plot is the most suitable one. In its behavior it closely follows the mobility gap  $E_\mu$ . Cody *et al.*,<sup>2</sup> on the other hand, pointed out that it is always possible to plot any root of  $\alpha$  and obtain a nearly linear variation with the energy. Several papers<sup>12-14</sup> suggested that an extrapolation of the nearly linear functional dependence of  $[\alpha(\hbar\omega)(\hbar\omega)]^{1/3}$  versus the photon energy is more suitable to define an optical gap ( $E_3$ ) than the Tauc plot. In this paper we use different criteria for determining optical gaps, and demonstrate that the Tauc plot is the most suitable one when compared with experimental results.

There is a large amount of experimental data on the optical properties of *a*-Si and *a*-Si:H.<sup>7</sup> Most of them demonstrate that the shape of the optical-absorption spectrum and the position of the Urbach edge are strongly dependent on the degree of thermal and structural disorder.<sup>2,15-19</sup> But it is very difficult in the experiment to separate those properties which are caused by defects and those which are the result of topological disorder. In contrast to the experimental investigations only a few calculations have been performed to understand the role that disorder plays in determining the shape of the optical-absorption spectrum. O'Leary and co-workers<sup>9,20,21</sup> and Zammit *et al.*<sup>22</sup> studied the influence of topological disorder on the optical properties of *a*-Si. Their investigations demonstrated that the width of the Urbach range increases with increasing degree of topological disorder. Simultaneously the value of the optical gap decreases. To study the influence of differently coordinated atoms on the properties of amorphous silicon, various structural models have been developed. Most of them are based upon molecular-dynamics simulations, and contain both dangling bonds and floating bonds. These structural models are able to address the question of which type of defect more strongly affects the electronic properties by calculating the local densities of states. However, they are not able to study the in-

fluence of the differently coordinated atoms on the optical properties, because these calculations are based on the total density of states. Here we present a detailed analysis of the optical properties of various structural models for *a*-Si and *a*-Si:H which only contain one type of defect. With these structural models we are able to differentiate between those properties in the optical spectrum which are caused by defects and those which are the result of topological disorder. It will be shown that topological disorder, hydrogen, and defects influence different parts of the optical-absorption spectrum, and that dangling bonds affect the optical properties more than floating bonds do.

The outline of the paper is as follows. Section II contains a short description of the different structural models and a discussion of their electronic structures. The optical properties are presented in detail in Sec. III. Conclusions are derived in Sec. IV.

## II. MODEL CONSTRUCTION AND ELECTRONIC PROPERTIES

We give a short description of the construction principles for the various structural models used in this paper, and briefly discuss their electronic properties together with the localization behavior of the states. This information is necessary to understand the optical processes in amorphous silicon, which depends explicitly on the details of the DOS. A detailed description was given in a previous paper.<sup>1</sup>

To simulate a continuous random network (CRN) we use the vacancy model of Duffy, Boudreaux, and Polk.<sup>23</sup> Topological disorder is introduced in this structural model by removing a given number of randomly chosen atoms from the diamond lattice. After each elimination step the four unsaturated bonds have to be reconnected by new bonds. The degree of disorder is characterized by the vacancy concentration  $c_f$ . This is the fraction of atoms which is removed from the regular lattice. To generate a structural model containing threefold-coordinated silicon atoms [dangling bonds (DB's)] we cut the longest bonds in a CRN and relax the resulting structure with the connectivity list. To introduce fivefold- and sixfold-coordinated atoms [floating bonds (FB's)], we remove four atoms which are second neighbors instead of only one atom from the regular lattice during each elimination step, because we have found that a large local vacancy concentration gives rise to overcoordinated silicon atoms. To generate an *a*-Si:H structure, from a defect structure we remove all silicon atoms with a coordination number different from 4 and saturate the resulting free bonds partially or completely with hydrogen.

The relaxation of the various structural models has been performed with a Monte Carlo procedure together with the Keating potential. The electronic properties are calculated with the tight-binding approximation. The parameters for the tight-binding Hamiltonian are taken from the work of Harrison<sup>24</sup> (*a*-Si) and Allan and Mele<sup>25</sup> (*a*-Si:H). To study the localization behavior and to determine the mobility edges  $E_V$  in the VB, and  $E_C$  in the CB, we use a method which was developed by Thouless, Edwards, and Licciardello.<sup>26,27</sup> We have considered four different vacancy concentrations ( $c_f = 0.025, 0.05, 0.10, \text{ and } 0.20$ ) to study the influence of topological disorder. To examine the changes in the properties

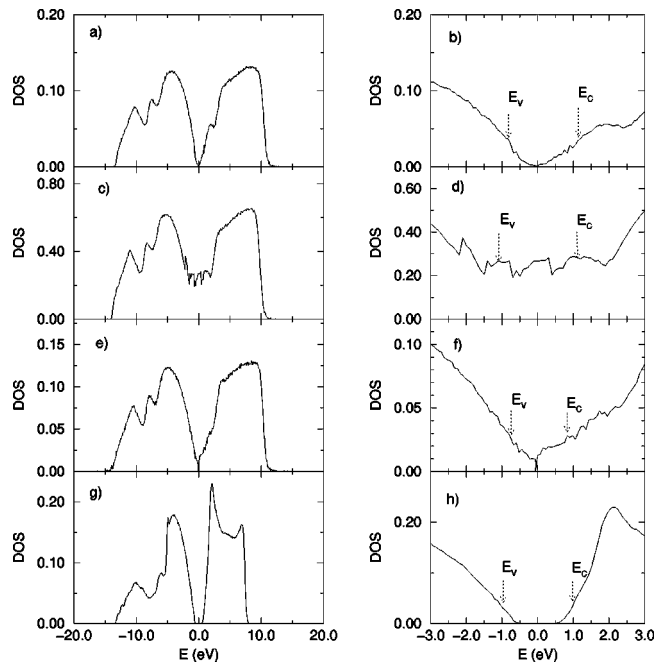


FIG. 1. Density of states for various structural models (3686 atoms): (a) and (b) CRN model ( $c_f=0.10$ ), (c) and (d) dangling-bond model ( $c_d=0.05$ ), (e) and (f) floating-bond model ( $c_d=0.05$ ), and (g) and (h)  $a$ -Si:H model ( $c_H=0.20$ ). The left-hand side presents the total DOS, and the right-hand side the region around the Fermi level with the mobility gaps indicated.

which are caused by different types of defects we compare amorphous structures with the same degree of topological disorder ( $c_f=0.10$ ) and vary the defect concentration from  $c_d=0.00$  to  $c_d=0.20$ .

Our investigations demonstrate that the principal structure of the DOS of the two energy bands is caused by the degree of topological disorder. The presence of different types of defects causes strong changes in the electronic properties only in the vicinity of the Fermi level. For the crystalline state the two energy bands show several characteristic features which are the result of the band structure in crystalline systems. Through the introduction of topological disorder, the long-range order disappears and the two energy bands lose their structure with increasing degree of disorder. Simultaneously the size of the energy gap decreases, but it only fills up for unrealistically high degrees of disorder. The structural properties of our CRN model show the best agreement with experiment for vacancy concentrations around  $c_f=0.10$ . For this degree of disorder the VB consists of two peaks, and the CB is nearly featureless [see Fig. 1(a)]. Via the introduction of different types of defects (DB's or FB's) the energy gap disappears and the number of electronic states in the vicinity of the Fermi level increases with increasing defect concentration. DB's induce more defect states than FB's do [see Figs. 1(b) and 1(d)]. The introduction of hydrogen removes all states around the Fermi level reintroducing a true gap between the VB and CB [see Fig. 1(c)]. The width of the gap increases with increasing hydrogen concentration, because silicon-silicon bonds are removed by stronger silicon-hydrogen bonds. The enlargement of this energy gap is mainly caused by a recession of the VB edge.

All structural models discussed in this paper show stron-

ger localization at the band edges of the CB than at the VB edges. The states in the interior of the two energy bands seem to be extended. In the defect models the states in the vicinity of the Fermi level induced by dangling bonds or floating bonds are completely localized as long as the defect concentration is small, i.e., the atoms participating in a defect are essentially isolated in the structure. For defect concentrations higher than  $c_d=0.10$  we find a small amount of extended states in the region of the Fermi level. The values of the mobility gaps,  $E_\mu$ , for the different structural models are listed in Table I. For the CRN model the width of the mobility gap decreases with increasing degree of topological disorder. In  $a$ -Si:H the mobility gap increases with the amount of hydrogen. For the dangling-bond model and the floating-bond model the values of the mobility gaps show no strong dependence on the defect concentration in the defect concentration range considered here. Stronger variations appear in the dangling-bond model than in the floating-bond model. The  $a$ -Si:H structure characterized by a hydrogen content of  $c_H=0.21$  shows a value of the mobility gap which is in good agreement with experimental results. This is not the case for the CRN model and the defect models. Their mobility gaps are too large.

### III. OPTICAL PROPERTIES

This section consists of two parts. The first one demonstrates the changes in the optical-absorption spectrum caused by the introduction of topological disorder and different types of defects. In the second part we analyze the changes with increasing disorder in the optical-absorption coefficient  $\alpha$ , and compare different criteria for determining band gaps from optical data.

Figure 2(a) demonstrates how topological disorder influences the optical-absorption spectrum. The shape is least affected in the high-energy range where it is comparable with the one found for the crystalline state. Whereas the absorption edge for the crystal terminates abruptly at about 4.5 eV, the presence of topological disorder leads to a shift of the absorption edge toward lower energies. This effect increases with an increasing degree of topological disorder. Simultaneously the value of the absorption coefficient increases as the number of possible band-to-tail and tail-to-tail transitions increases. With an increasing degree of topological disorder the absorption edge obtains a smaller gradient. For all degrees of topological disorder the optical-absorption spectrum contains different ranges of the energy dependence. For photon energies below 2.0 eV,  $\log_{10} \alpha$  increases more or less linearly, which indicates an exponential dependence on the energy. The logarithm of the absorption coefficient is nearly constant for photon energies higher than 6.0 eV. In the energy range between 2.0 and 6.0 eV,  $\alpha$  shows no specific dependence on the energy. A broader transition region between the exponential part of the optical-absorption spectrum and the high-energy range was also observed in various experiments on  $a$ -Si than  $a$ -Si:H.<sup>7</sup>

In contrast to the CRN model, the transitions between the different parts of the optical spectrum of the dangling bond model become less obvious with increasing defect concentration. The absorption spectrum for this structural model is displayed in Fig. 2(b). In contrast to the CRN model, the

TABLE I. Band gaps obtained by various methods for the different structural models (in eV).

CRN model	$c_f=0.025$	$c_f=0.05$	$c_f=0.10$	$c_f=0.20$	
$E_\mu$	2.8	2.5	2.0	0.8	
$E_{Tauc}$	2.2	2.1	1.7	1.3	
$E_3$	1.8	1.5	1.1	0.6	
$E_{04}$	3.1	2.6	2.0	1.4	
DB model	$c_d=0.00$	$c_d=0.02$	$c_d=0.04$	$c_d=0.11$	$c_d=0.20$
$E_\mu$	2.0	2.5	2.2	2.0	2.1
$E_{Tauc}$	1.9	1.9	1.7	1.3	1.2
$E_3$	1.0	1.1	0.6	0.8	0.4
$E_{04}$	2.0	1.9	1.7	0.4	0.2
FB model	$c_d=0.00$	$c_d=0.02$	$c_d=0.04$	$c_d=0.11$	$c_d=0.20$
$E_\mu$	2.0	1.8	2.0	1.0	1.0
$E_{Tauc}$	1.8	1.6	1.5	1.6	1.3
$E_3$	1.0	0.7	0.6	0.5	0.4
$E_{04}$	1.8	1.7	1.7	1.4	1.2
<i>a</i> -Si:H model	$c_H=0.00$	$c_H=0.06$	$c_H=0.12$	$c_H=0.21$	$c_H=0.42$
$E_\mu$	1.0	1.2	1.3	1.8	2.4
$E_{Tauc}$	1.2	1.4	1.5	1.9	2.2
$E_3$	0.6	0.8	1.0	1.5	1.9
$E_{04}$	1.0	1.3	1.6	2.0	2.3

optical spectrum of the dangling-bond model consists of three parts, because threefold-coordinated atoms give rise to absorption processes below the Urbach range (tail absorption). Whereas the optical spectrum in the high-energy range above 4 eV is nearly unaffected by the presence of dangling bonds, the absorption behavior in the other regions is quite different from that of the CRN model. The intensity of the absorption below the Urbach edge increases dramatically with increasing defect concentration. This effect is stronger in the range of tail absorption than the corresponding effect in the Urbach range. Furthermore, the increase of the absorption edge becomes less steep with an increasing concentration of dangling bonds.

For defect concentrations smaller than  $c_d=0.05$ , the tail absorption behavior shows no specific structure. For larger dangling-bond concentrations we observe the formation of an additional peak in this energy range with a maximum close to the Fermi level. The width of this peak increases with increasing amount of threefold-coordinated atoms. Simultaneously the width of the Urbach range decreases. In the case when  $c_d$  exceeds 0.10, the value of the absorption coefficient in the range of the tail absorption is in some cases higher than  $10^4 \text{ cm}^{-1}$ , which indicates the presence of extended states in the range of the tail absorption. This result agrees with our earlier investigations about the localization behavior of electronic states in *a*-Si and *a*-Si:H.<sup>1</sup> There we find the presence of extended states in the vicinity of the Fermi level for the case where dangling bonds are no longer isolated in the structure.

Compared to the dangling-bond model, the changes in the optical properties caused by the presence of floating bonds

are smaller [see Fig. 2(d)]. Analogous to the structural model for threefold-coordinated atoms, the optical spectrum of the floating-bond model consists of three parts, and the absorption below the Urbach edge increases with increasing amount of fivefold- and sixfold-coordinated atoms. In contrast to the dangling-bond model, the absorption behavior in the range of tail absorption shows no specific structure for all defect concentrations investigated here. We only observe a shoulder which extends from about  $E=0.0$  eV to the beginning of the Urbach range at about 1.0 eV. The intensity of the absorption in this energy range increases in a nearly monotonic fashion with an increasing amount of floating bonds. The width of the exponential part of the optical spectrum shows no strong dependence on the defect concentration. The value of the absorption coefficient in the range of tail absorption is always smaller than for the dangling-bond model, and never exceeds  $10^4 \text{ cm}^{-1}$ . That is, all electronic states in the vicinity of the Fermi level caused by floating bonds are localized. Analogous to the structural models mentioned above, the increase of the absorption edge becomes less steep with increasing amount of fivefold- and sixfold-coordinated atoms.

Up to now we have only discussed the influence of topological disorder and different types of defects on the optical properties. Let us now turn to the question how these properties change when defects are partially or completely saturated by hydrogen. Figure 3 demonstrates the changes in the optical absorption spectrum when dangling bonds are partially passivated with hydrogen. In contrast to the pure dangling-bond model, the absorption behavior of an *a*-Si:H structure with defects shows no specific features in the range

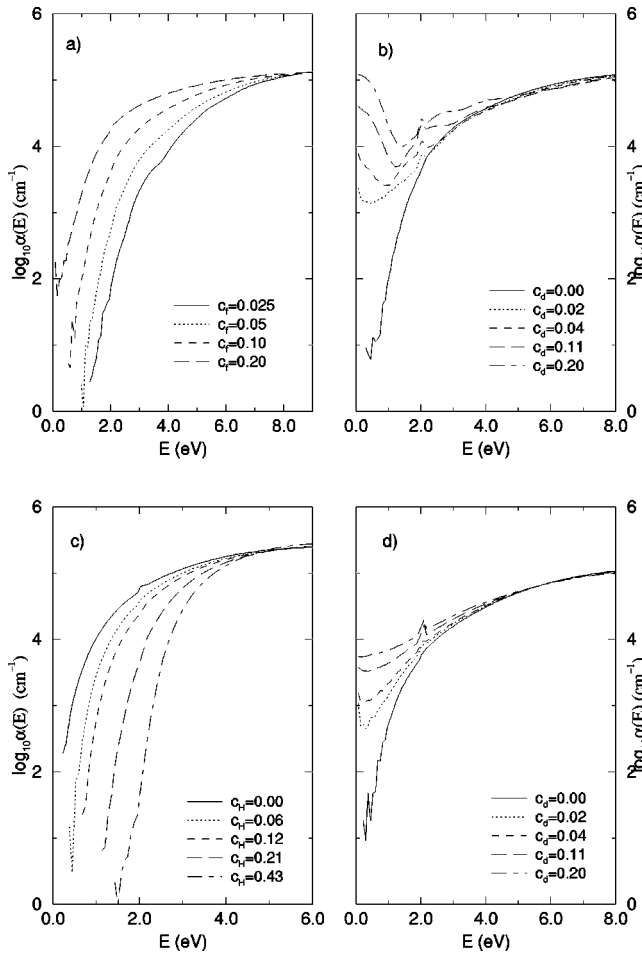


FIG. 2. Optical-absorption coefficient  $\alpha$  as a function of the photon energy for various structural models (5000 atoms): (a) CRN model, (b) dangling-bond model, (c) *a*-Si:H model, and (d) floating-bond model.

of tail absorption. The different regions of the optical-absorption spectrum are clearly visible, independent of the defect concentration. With an increasing amount of hydrogen and a decreasing defect concentration, the intensity of the tail absorption decreases and  $\alpha$  drops. Simultaneously the absorption edge shifts to higher energies. This behavior of the optical-absorption spectrum was also observed in the experiment, when the pressure of hydrogen was increased during the growth process.

Figure 2(c) displays the optical spectrum of various defect free *a*-Si:H structures. Analogously to the CRN model, the principal structure of the optical spectrum is nearly independent of the amount of hydrogen and shows no tail absorption, because all silicon atoms are fourfold coordinated. With an increasing hydrogen concentration the Urbach edge shifts to higher energies. This result demonstrates that the increase of the optical gap with the amount of hydrogen is mainly the result of an alloy formation similar to the situation in *a*-SiC:H, where  $E_g$  also varies linearly with the hydrogen concentration and is not due to the reduction in the number of defects, an assumption which is often found in the literature. In contrast to the other structural models discussed above, the absorption edge rises steeper with an increasing amount of hydrogen. The optical-absorption spectrum of our *a*-Si:H model shows the best agreement with experiment for

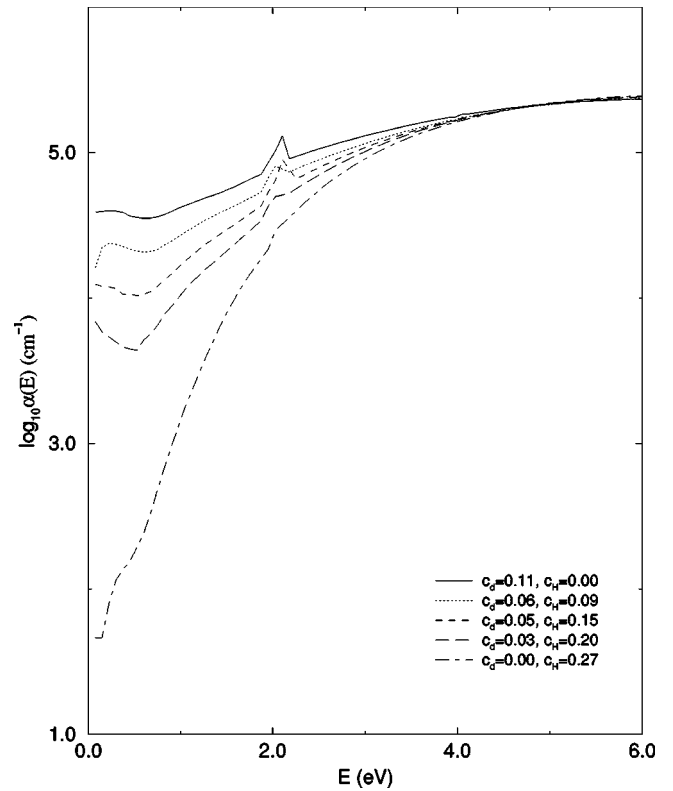


FIG. 3. Optical-absorption coefficient  $\alpha$  for *a*-Si:H structures containing dangling bonds (5000 atoms).

hydrogen concentrations between  $c_H=0.12$  and 0.21.

So far we have only described the changes in the structure of the optical spectrum caused by disorder and defects. Next we will discuss the changes in the optical gap with increasing disorder. In Fig. 4 we plot  $\sqrt{\alpha(\hbar\omega)\hbar\omega}$  versus the photon energy for the CRN model, the dangling-bond model, and the *a*-Si:H model. The Tauc plot for the floating-bond model is not shown, because for this structural model the changes in the optical gaps are too small to be visualized. It can be seen that for high energies ( $E \geq 1.5$  eV)  $\sqrt{\alpha(\hbar\omega)\hbar\omega}$  exhibits an essentially linear dependence on the energy, i.e., Tauc absorption edges are observed. Extrapolating this high-energy Tauc absorption behavior to zero absorption gives the values of the optical gap  $E_{Tauc}$  listed in Table I.

For the CRN model the Tauc gap decreases nearly linearly with an increasing degree of topological disorder. The introduction of hydrogen in *a*-Si widens the optical gap. This effect also increases linearly with an increasing amount of hydrogen, as observed experimentally.<sup>8</sup> Comparing the optical gaps of the CRN model and the *a*-Si:H model with the mobility gaps  $E_\mu$  obtained in our earlier work, we find an almost parallel development with an increasing degree of disorder and an increasing amount of hydrogen. This is not always the case for the two defect structural models. There the differences between the optical gaps and the mobility gaps increase with the defect concentration. Whereas the mobility gaps show no specific dependence on the defect concentration, the values of the optical gaps for the defect structural models decrease with increasing defect concentration. This effect is stronger for the dangling-bond model than for the floating-bond model. Compared to the mobility gaps the values of the optical gaps obtained by the Tauc plot are in

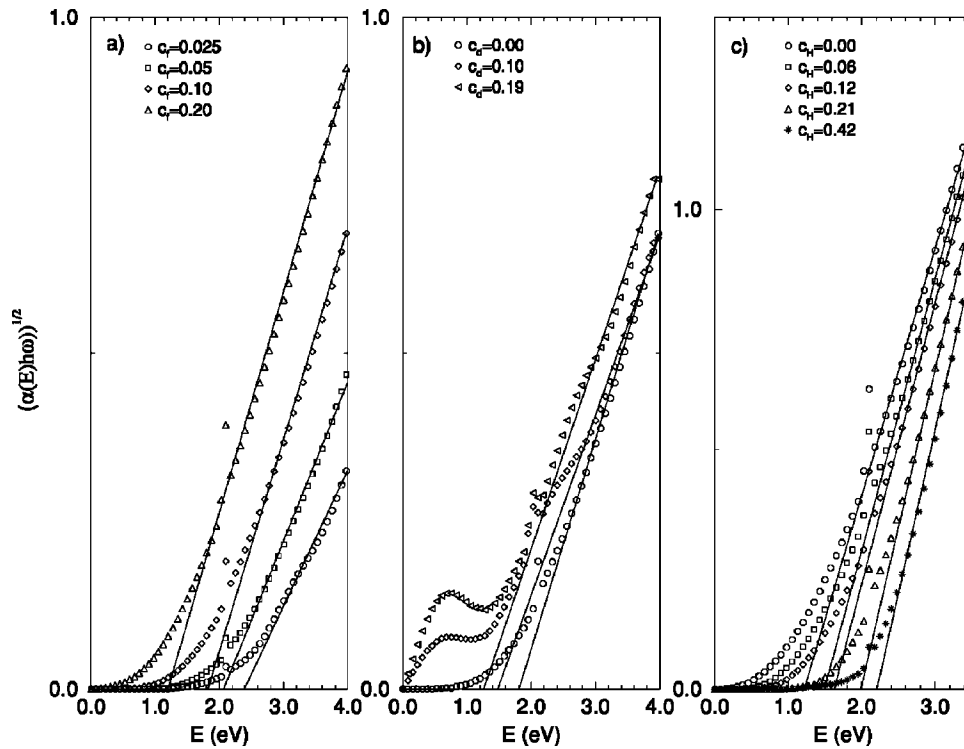


FIG. 4. The square root of the optical-absorption coefficient vs the photon energy for various structural models (5000 atoms). The dotted lines show the Tauc extrapolation.

general 0.2–0.4 eV smaller. This result was also found in other theoretical investigations, and indicates that the exponential part of the optical-absorption spectrum begins below the mobility edge, a question which has been discussed controversially and unresolved till now. From our calculations it emerges clearly that the absorption begins below the mobility edge.

Finally we would like to discuss the accuracy of the different methods that are in use to determine band gaps from optical data. Table I summarizes the optical gaps for the different structural models. A comparison demonstrates that all criteria are able to describe the principal changes in the optical gaps caused by disorder or by defects correctly. That is, through the introduction of topological disorder and different types of defects, the optical gap decreases. The presence of hydrogen, on the other hand, widens the optical gap. In general, the values of the optical gaps obtained by the various methods increases in the following order:  $E_3 \leq E_{Tauc} \leq E_\mu \leq E_{04}$ . This relation was also found by Jackson *et al.*,<sup>5</sup> who calculated the optical properties from experimental DOS measurements. In most cases the optical gaps using Tauc's definition show the best agreement with experimental results and are comparable with the mobility gaps. This is the only method which gives reasonable values of the optical gap for all structural models, independent of the degree of disorder and the defect concentration. In particular, the  $E_3$  values obtained by the  $[\alpha(\hbar\omega)\hbar\omega]^{1/3}$  plot versus the photon energy give optical gaps which are substantially smaller than the experimental values for the two defect structural models. The criterion of the isoabsorption gap  $E_{04}$  should not be used for determining an optical gap for structures with high concentrations of dangling or floating bonds. In these cases we find a strong correlation between the region

of tail absorption and the Urbach range, which complicates the definition of an optical gap.

#### IV. CONCLUSION

In this paper we have presented the optical properties of various structural models for *a*-Si and *a*-Si:H. We have demonstrated how topological disorder, hydrogen, dangling bonds, and floating bonds affect the structure of the optical-spectrum, and the position of the Urbach edge. The latter is mainly caused by the degree of topological disorder and the amount of hydrogen. Topological disorder leads to a broadening of the exponential part of the optical-absorption spectrum and reduces the magnitude of the optical gap. The introduction of hydrogen shifts the absorption edge toward higher energies, which causes a widening of the optical gap. The presence of defects gives rise to tail absorption and increases the absorption below the high-energy range. These effects are stronger in the dangling-bond model than in the floating-bond model. The results presented in this paper demonstrate that electronic and optical properties are both suitable to study the influence of disorder and different types of defects on the properties of amorphous semiconductors.

#### ACKNOWLEDGMENTS

The authors acknowledge financial support from the Deutsche Forschungsgemeinschaft, and partial support by the Fonds der Chemischen Industrie. They also thank the computing center of the Technical University of Braunschweig and the HLRZ Jülich for the supply of computing time.

- <sup>1</sup>S. Knief, W. von Niessen, and Th. Koslowski, *Phys. Rev. B* **58**, 4459 (1998).
- <sup>2</sup>G. D. Cody, T. Tiedje, B. Abeles, B. Brooks, and Y. Goldstein, *Phys. Rev. Lett.* **47**, 1480 (1981).
- <sup>3</sup>F. Urbach, *Phys. Rev.* **92**, 1324 (1953).
- <sup>4</sup>G. D. Cody, *Hydrogenated Amorphous Silicon*, edited by J. I. Pankove, *Semiconductors and Semimetals*, Vol. 21B (Academic, New York, 1984), p. 11.
- <sup>5</sup>W. B. Jackson, S. M. Kelso, C. C. Tsai, J. W. Allen, and S.-J. Oh, *Phys. Rev. B* **31**, 5187 (1985).
- <sup>6</sup>W. B. Jackson, C. S. Tsai, and S. M. Kelso, *J. Non-Cryst. Solids* **77/78**, 281 (1985).
- <sup>7</sup>L. Ley, in *The Physics of Hydrogenated Amorphous Silicon II*, edited by J. D. Joannopoulos and G. Lucovsky (Springer, Heidelberg, 1984).
- <sup>8</sup>N. F. Mott and E. A. Davis, *Electronic Processes in Non-Crystalline Materials*, 2nd ed. (Clarendon, Oxford, 1979).
- <sup>9</sup>S. K. O'Leary, S. Zukotynski, and J. M. Perz, *Phys. Rev. B* **52**, 7795 (1995).
- <sup>10</sup>S. K. O'Leary, S. Zukotynski, and J. M. Perz, *Phys. Rev. B* **51**, 4143 (1995).
- <sup>11</sup>J. Tauc, R. Grigorivici, and A. Vancu, *Phys. Status Solidi* **15**, 627 (1966).
- <sup>12</sup>R. H. Klazes, X. van den Broeck, J. Bezemer, and S. Radelucek, *Philos. Mag. B* **45**, 377 (1982).
- <sup>13</sup>V. N. Novikov, A. P. Sokolov, O. A. Golikova, V. Kh. Kudoyatova, and M. M. Mezdrogina, *Fiz. Tverd. Tela (Leningrad)* **32**, 1515 (1990) [*Sov. Phys. Solid State* **32**, 884 (1990)].
- <sup>14</sup>A. P. Sokolov, A. P. Shebanin, O. A. Golikova, and M. M. Mezdrogina, *J. Phys. Condens. Matter* **3**, 9887 (1991).
- <sup>15</sup>A. R. Zanatta, M. Mulato, and I. Chambouleyron, *J. Appl. Phys.* **84**, 5184 (1998).
- <sup>16</sup>R. A. Street, T. M. Searle, I. G. Austin, and R. S. Sussmann, *J. Phys. C* **7**, 1582 (1974).
- <sup>17</sup>T. Tiedje and J. M. Cebulka, *Phys. Rev. B* **28**, 7075 (1983).
- <sup>18</sup>P. D. Persans, A. F. Ruppert, S. S. Chan, and G. D. Cody, *Solid State Commun.* **51**, 203 (1984).
- <sup>19</sup>G. D. Cody, *J. Non-Cryst. Solids* **141**, 3 (1992).
- <sup>20</sup>S. K. O'Leary, S. R. Johnson, and P. K. Lim, *J. Appl. Phys.* **82**, 3334 (1997).
- <sup>21</sup>S. K. O'Leary, S. Zukotynski, and J. M. Perz, *J. Non-Cryst. Solids* **210**, 249 (1997).
- <sup>22</sup>U. Zammit, K. N. Madhusoodanan, F. Scudieri, F. Mercuri, E. Wendler, and W. Wesch, *Phys. Rev. B* **49**, 2163 (1994).
- <sup>23</sup>M. G. Duffy, D. S. Boudreaux, and D. E. Polk, *J. Non-Cryst. Solids* **15**, 435 (1974).
- <sup>24</sup>W. A. Harrison, *Electronic Structure and the Properties of Solids* (Freeman, San Francisco, 1980).
- <sup>25</sup>D. C. Allan and E. J. Mele, *Phys. Rev. B* **31**, 5565 (1985).
- <sup>26</sup>D. C. Licciardello and D. J. Thouless, *J. Phys. C* **8**, 5157 (1975); **11**, 925 (1978).
- <sup>27</sup>J. T. Edwards and D. J. Thouless, *J. Phys. C* **5**, 807 (1972).